NASA TECHNICAL TRANSLATION NASA TT F-16,187

# STUDIES RELATIVE TO AN INDUCTION PRESSURIZED TRANSONIC WIND TUNNEL A. AIR PUMP PERFORMANCE; CIRCUIT LOSSES

C. Quemard, A. Mignosi, A. Seraudie

Translation of "Etudes Relatives a une Soufflerie Transsonique Pressurisee a Induction. A) Performances des trompes; pertes du circuit," O.N.E.R.A., Centre d'Etudes de Recherches de Toulouse, D.E.R.A.T. Technical Note No. 5/5006 DN, July, 1974, 28 pp.

(NASA-TT-F-16187) STUDIES RELATIVE TO AN INDUCTION PRESSURIZED TRANSONIC WIND TUNNEL. A: AIR PUMP PERFORMANCE; CIRCUIT LOSSES (Kanner (Leo) Associates) 33 p HC $3.75 CSCL 14B G3/09

N75-21291

Unclas 18678



NATIONAL AERONAUTICS AND SPACE ADMINISTRATION
WASHINGTON, D.C. 20546 MARCH 1975

STANDARD TITLE PAGE

| | | |
|---|---|---|
| 1. Report No. NASA TT F-16,187 | 2. Government Accession No. | 3. Recipient's Catalog No. |
| 4. Title and Subtitle STUDIES RELATIVE TO AN INDUCTION PRESSURIZED TRANSONIC WIND TUNNEL A. AIR PUMP PERFORMANCE; CIRCUIT LOSSES | | 5. Report Date March 1975 |
| | | 6. Performing Organization Code |
| 7. Author(s) C. Quemard, A. Mignosi, A. Seraudie | | 8. Performing Organization Report No. |
| | | 10. Work Unit No. |
| 9. Performing Organization Name and Address Leo Kanner Associates Redwood City, California 94063 | | 11. Contract or Grant No. NASw-2481 |
| | | 13. Type of Report and Period Covered Translation |
| 12. Sponsoring Agency Name and Address National Aeronautics and Space Administration, Washington, D. C. 20546 | | 14. Sponsoring Agency Code |

15. Supplementary Notes

Translation of "Etudes Relatives a une Soufflerie Transsonique Pressurisee a Induction. A) Performances des trompes; pertes du circuit." O.N.E.R.A., Centre d'Etudes de Recherches de Toulouse, D.E.R.A.T. Technical Note No. 5/5006 DN, July 1974, 28 pp.

16. Abstract

This note summarizes the performance tests of the $T'_2$, a prototype transonic induction wind tunnel. It is shown that there are advantages in using an air jet pump incorporating guide vanes at the first elbow of the wind tunnel with injection at $M_j = 1.6$ at the trailing edge. The solutions adopted for removing the drive fluid are presented.

| | |
|---|---|
| 17. Key Words (Selected by Author(s)) | 18. Distribution Statement Unclassified-Unlimited |

| | | | |
|---|---|---|---|
| 19. Security Classif. (of this report) | 20. Security Classif. (of this page) | 21. No. of Pages | 22. Price |
| Unclassified | Unclassified | 27 | |

TABLE OF CONTENTS

STUDIES RELATIVE TO AN INDUCTION PRESSURIZED TRANSONIC WIND TUNNEL
A. AIR PUMP PERFORMANCE; CIRCUIT LOSSES

C. Quemard, A. Mignosi, A. Seraudie

## 1. Introduction

The $T'_2$ prototype wind tunnel was installed at DERAT for the /2* purpose of providing information necessary for the design of the $T_2$ wind tunnel, and, at a later date, of the European transonic wind tunnel IDT (Injection Driven Tunnel).

This involves a return circuit that can be pressurized up to 5 bars. The "driver" of the flow is an air jet pump. This type of wind tunnel is not new, but recent requirements bearing on either the energy dissipation or the flow quality have led us to undertake a systematic study.

Different aspects have been considered. The first, which is the subject of this note, concerns the performance of this type of wind tunnel. A second note describes the initial motion of the flow and the measurements of the characteristic magnitudes (pressures, impact temperature) recorded during the first tenths of a second of an air blast.

## 2. Calculations of the Injection Flow

The drive unit of an induction wind tunnel is the injector which delivers a high pressure air jet in order to drive the principal air flow and to provide the energy necessary to compensate for the circuit losses. The calculation for this injector can be carried out starting from the overall equations of conservation of momentum, mass and energy [1].

*Numbers in the margin indicate pagination in the foreign text.

Let us consider an air jet assumed to be uniform and having subscript (j) and a forced airflow having subscript (1). These two airflows are mixed so as to result in a complex airflow that can be replaced by an equivalent airflow that is assumed uniform with subscript (m). The conservation laws may then be written (plate 1):

Conservation of mass:

$$(1-\tau)\,\rho_1 u_1 + \rho_J u_J \tau = \rho_m u_m$$

Conservation of momentum:

$$(1-\tau)(p+\rho u^2)_1 + \tau (p+\rho u^2)_J = (p+\rho u^2)_m$$

Conservation of energy:

$$hi_1 = hi_J = hi_m$$

$hi_1 = hi_j = hi_m$, assuming that the initial flows are at equal generative temperatures. $\tau$ represents the ratio of the injector cross section to the total cross section of the mixer.

The preceding system can be put in a more manageable form by using the known functions of the Mach number:

/3

$$\Sigma(M) = \frac{1}{M}\left[\frac{1+\frac{\gamma-1}{2}M^2}{\frac{\gamma+1}{2}}\right]^{\frac{\gamma+1}{2(\gamma-1)}} = \frac{S}{S^*}$$

$$\varpi(M) = \left(1+\frac{\gamma-1}{2}M^2\right)^{-\frac{\gamma}{\gamma-1}} = \frac{P}{P_i}$$

$$\phi(M) = (1+\gamma M^2)\,\frac{1}{M\sqrt{1+\frac{\gamma-1}{2}M^2}}$$

We thus obtain:

$$\phi(M_m) = \frac{\phi(M_1) + \mu^{-1}\phi(M_J)}{1+\mu^{-1}}$$

$$\frac{P_{im}}{P_{i1}} = (1+\mu^{-1})(1-\tau)\,\frac{\Sigma(M_m)}{\Sigma(M_1)}$$

with $\mu^{-1} = \dfrac{\rho_J u_J \tau}{\rho_1 u_1 (1-\tau)} = \dfrac{q_J}{q_1}$ $\dfrac{\text{flow rate of injected air}}{\text{flow rate of forced air}}$

Let $\dfrac{P_{iJ}}{P_{i1}} = \mu^{-1}\cdot\dfrac{1-\tau}{\tau}\cdot\dfrac{\Sigma(M_J)}{\Sigma(M_1)}$

The unknowns of this system are seven in number:

$$M_1,\ M_j,\ M_m,\ \tau,\ \mu^{-1},\ \frac{P_{im}}{P_{i1}},\ \frac{P_{iJ}}{P_{i1}}$$

It is thus necessary to fix 4 parameters. It is logical to choose the injector geometry ($\tau$) and the characteristics of the initial flow ($M_1$, $M_j$, $\frac{P_{iJ}}{P_{i1}}$ ). We then deduce $\mu^{-1}$, $M_m$, $\frac{P_{im}}{P_{i1}}$

The results of the calculations are displayed in plates 2,3,4, and 5. In plate 2 we have shown, for $M_j = 1$, $\lambda = \tau^{-1} = 20$, both the injector efficiency E, defined as $\mu\frac{\delta P_i}{P_i}\left(=\mu\frac{P_{im}-P_{i1}}{P_{i1}}\right)$, as a function of $M_1$, and the ratio of the flow rates $\mu^{-1}$ as a function of $\frac{\delta P_i}{P_i}$.

We observe that the efficiency is an increasing function of $M_1$, the Mach number for forced flow, except in the case that $P_j = P_1$, that is, for an adjusted jet: there a maximum of efficiency occurs for $M_1 \simeq 0.5$.

The adjustment presents a priori certain technical or aerodynamic advantages about which we shall have more to say later. Let us notice however that the dependence on $\frac{\delta P_i}{P_i}$ is a weak one. In /4
order to make up for the higher load losses it is necessary, for a given value of $M_1$, to use stronger and stronger jet pressures.

Plate 3 shows that the efficiency is roughly independent of $\lambda$.

Plate 4 shows the strong influence of the Mach number $M_j$ on the efficiency, particularly for the small pressure ratios $Pi_j/Pi_1$, and thus for the modified version.

With $M_J = 1.6$ an air flow can be driven at $M_1 = 0.6$ with load losses in one circuit on the order of 10%. Let us then underline the fact that the increase in efficiency observed at $M_j = 1.6$ is made however at the expense of the pressure ratio $Pi_j/Pi_1$.

Plate 5 summarizes for the case of the adjusted configuration the influence of $M_j$ on efficiency and of $M_1$ and $\lambda$ on the input flow rate for given load losses.

Two experimental verifications of these calculations have been indirectly obtained.

The first (see plate 14) supposes that the load losses in the circuit are independent of the value of $\lambda$ for the injector. In this case, knowing the input flow for the adjusted configuration ($\mu$) and the Mach number of the forced low ($M_1$), we can deduce from the theoretical curves the load losses $\delta P_i / P_i$ of the circuit corresponding to this Mach number. Knowing the losses, for a given value of $M_1$, we can deduce in turn the flow rates through the air pump for $\lambda = 20$ and 40. The agreement between the calculations and the experiment is very satisfactory.

The second verification was obtained by varying the load losses of the circuit in a known way. We have determined that the grids of the plenum chamber give rise to a load loss of 0.6% per element. Suppression of 3 grids thus reduced the losses, equal to 11% for $M_v = 0.8$ according to the calculations, to 11 – 1.8 = 9.2%. The increase in input flow had to be 11.5% according to the calculations, which the experiment verified.

### 3. T'$_2$ Circuits. Peripheral and Elbow Injection Systems at $M_j = 1$

In practice two injection systems are used (plate 6):

– Peripheral injection which is made through a slit along the four sides of the duct;

– central injection at the trailing edge of the intake guide vanes of the first elbow following the test flow region.

The characteristics of the injectors that have been used are the following: /5

| | $M_j$ | $\lambda$ |
|---|---|---|
| peripheral injection | 1 | 23 |
| elbow injection | 1<br>1.6 | 30*<br>20 to 60 |

(* In fact, for $M_j = 1$, the slits along the partition walls made it possible to reach $\lambda = 23$).

A comparison of the two systems supposes that the problem of removing the injected air has first been settled. Depending on the site of removal, the overall efficiency of the system: injector + wind tunnel, will be rather high.

Plate 7 shows, for the case of peripheral injection, that the removal of the air between the region of air flow and the injector leads to an increase in flow rate $\left(\frac{Q_I}{Q_V} = \frac{P_{iI}}{P_{iV}}\right)$ of 32% between M = 0.3 and 0.7, as compared with a removal site located in the return circuit (after the second elbow). A detailed analysis of the experiments shows that this result is easily explained by the fact that for Mach number $M_1$ of the forced flow the losses in the wind tunnel are approximately the same, but removal of air between the air flow region and the injector acts like a diffuser, and at $M_1$ it corresponds to an $M_v$ (the Mach number in the air flow region) given by the ratio of flow rates. It may thus be said that, for a given $M_v$, the injector must drive less air if the removal of the injected air is made upstream from the injector.

Let us note that the peripheral injector blocks the flow of air for the ratio $Pi_j/Pi_v > 6$ by forming a constriction due to the bursting of jets at the exit of the injection slits.

The following comparisons between peripheral injection and injection with elbow vanes will henceforth be made on the basis of the removal of air taking place between the air flow region and the injector, unless indicated to the contrary.

Plate 8 gives the performance obtained with the two types of injection at $M_j = 1$. The mixer in the two cases is of optimal length, and in the case of elbow injection the wind flow through the lateral slits has been suppressed (see plate 10).

An appreciable increase in injected flow rate may be noted, for a given $M_v$, with elbow injection (about 25%).

This result may be explained in part by the length of the /6
mixer necessary for optimum operation of the two types of injection.

Figure 9 shows that the optimum ratio L/H of the length to height of the mixer is on the order of 6 for peripheral injection and 2 for elbow injection. Let us note that a maximum for the Mach number would be obtained for the same L/h, h representing the distance between injection slits. Thus, an increase in the number of jets involves a reduction of the length of the mixer and an appreciable improvement in the efficiency of the combination: air pump plus wind tunnel.

Finally figure 10 shows that the division of the jet streams in the case of injection by vanes has a strong influence on performance. The figure on the right shows that the wind flow through the lateral slits decreases the efficiency of the air pump, irrespective of the feed pressure of the slits. The one on the left shows that the outside vanes of the elbow (2 and 3) work better than the inside vane (1). In the two cases shown this can be explained by the fact that the lateral slits like the vane 1 blow in an airflow that is degraded either by the boundary limit or by a separation of layers.

## 4. Detailed Study of T'$_2$ With Elbow Injection at $M_j = 1.6$

Having determined the location of the removal site and the mode of injection, we carried out a more detailed study of injection by vanes at $M_j = 1.6$. Indeed it has already been remarked that this Mach number for injection makes it possible to obtain adequate pressure ratios while still retaining the adjusted jets. A priori the adjustment would offer the advantage of decreasing the jet noise [2] and considerably reducing the mechanical constraints at the trailing edge of the vanes.

The system diagram for the T'$_2$ wind tunnel in this version is reviewed in figure 11.

Injection is made downstream from the first diffuser by two vanes each having four nozzles.

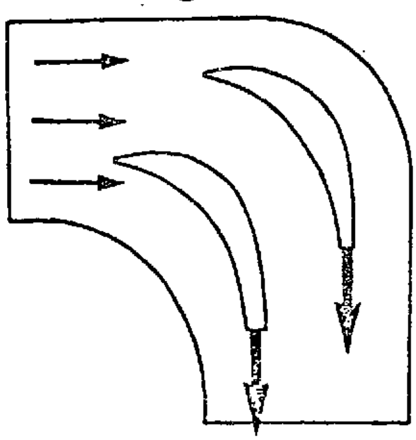

Exit view of the elbow.

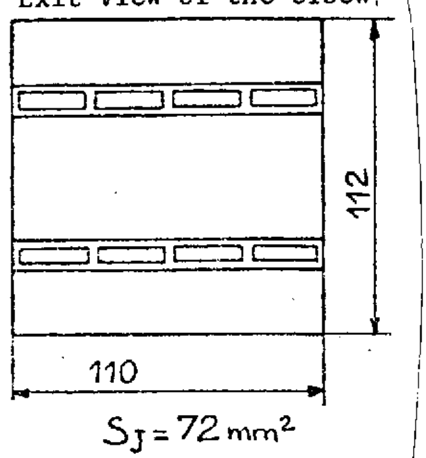

The injection area for a nozzle unit at $M_j = 1.6$ is: /7
$S_j = 72\ mm^2$.

The area of the mixer: 12300 $mm^2$:

The ratio $\lambda = Sm/Sj$ may vary by integer values from 170 to 21, the smallest value corresponding to eight nozzles in operation.

By virtue of this setup, it is possible to retain the adjusted jets by varying $\lambda$ with the Mach number of the air flow.

In view of the importance of the injection system to the $T_2$ wind tunnel project, a detailed examination has been carried out of the feed pressures and of the nozzles.

Included with the vanes, upstream from the constriction, in the collector region, are some filters whose purpose is to make the generation pressure uniform. Plate 12 indicates the evolution of the generation pressures from the feed valve up to the collector. The filters now being used cause a load loss on the order of 30%. That caused by flexible parts of the feed unit is negligible.

The measurement of the Mach number $M_j$ at the nozzle exit has been made in two ways:

– starting from the ratio of the static pressure $P_{S\hat{A}}$ at the exit of the vane to the impact pressure $P_{ij}$;

– starting from the ratio of the impact pressure measured by a probe in the exit plane to the pressure $P_{ij}$.

The results are given in plate 13. The average Mach number obtained is seen to lie around 1.55; a correct result will take account of the fact that the nozzles have not been corrected for the displacement of the boundary layer.

Fig. 14 shows the effect of varying $\lambda$ on performance, as compared with calculations for the air pump. To be sure, it must be remarked that if increase in the value of $\lambda$ is advantageous, it also involves a significant increase in the generation pressure of the jet, and hence of the storage pressure in the reservoirs. A balance sheet for the overall energy remains to be made taking into account the work necessary to assure adequate storage pressure, as well as the relaxation losses and the Joule-Thompson effect, etc....

Be that as it may, let us recall that the adjusted configuration makes it possible to avoid a lot of work as regards the vanes in particular.

In this plate we also observe the influence of the choice of the vanes to insure that $\lambda$ = 40. The inside vane does not work as well as the outside vane, as was seen above. The best choice is quite clearly to inject by two vanes, which insures a more efficient mixture through combination of the jets.

The first diffuser leads to a recompression of the flow tanks /8
on the one hand to a light geometric diffusion (10%), and on the other hand to removal of the injected flow stream. It is made of porous sheets (METAFRAM BM 50) on four sides.

The problem with such a diffuser is the regulation of the flow at each point to avoid recirculations through the sintered partition walls. Indeed, the pressure inside the chamber is uniform while the pressure along the diffuser increases. The discharge flow has a tendency to cross the porous plates in the region where the pressure difference is highest, that is, at the end of the diffuser.

The solution is to obstruct the plate in a gradual way going from upstream to downstream, so that the flow per unit length of diffuser remains approximately constant. A simple calculation, starting from an initial distribution of Mach numbers in the diffuser, makes it possible to determine the proportion of surface area to be blocked as a function of the abscissa. A practical solution has been carried out using slender longitudinal stops.

The experimental results are shown in Figures 15 and 16. Figure 15 shows that the configuration of the diffuser has allowed us to obtain a correct recompression and an increase in flow rate of more than 15%. Figure 16 shows the distributions of Mach number and of pressure for different values of Mach numbers in the flow region, that is to say, different values of $P_{ij}$. It is seen that the pressures in the chamber are practically always less than the pressures in the diffuser.

A last improvement test for this diffuser consisted of shortening it from 480 to 130 mm in the hope of thereby reducing the thickness of the boundary layer and thus of the losses in this diffuser, while maintaining a very acceptable geometric diffuser angle (2°). Figure 17 does indeed show an increase in flow rate on the order of 7%. In this plate there is also summarized the different stages of improvement in the performance of $T'_2$. It is seen that with respect to peripheral injection, the intake rate has been practically divided by two for a Mach number in the neighborhood of 0.9.

The second diffuser is made of porous sheets like the first diffuser. Chambers enclose these elements, removal of air being taken care of by the exit valves.

The change in circular cross-section carried out in the layout at the level of the mixer can equally well be done along the whole length of the second diffuser.

The intake in the second diffuser, according to the calculations of load loss through the development of the boundary layer at the partition walls of the wind tunnel, may a priori lead to an improvement in performance. In fact, since the decrease of the load losses is especially sensitive at the lower percentages to the intake flow rate, the removal of the flow at two places of the circuit (first and second diffusers) seemed to bring better results, despite the opposite effect due to the probable increase of the forced flow /9 by the air pump.

The experiment shows that if indeed there does exist a slight decrease of load losses in the circuit, it is not sufficient to counterbalance the lack of diffusion between the region of flow and the injector elbow. Curve 18 shows the Mach number in the flow region obtained for a constant flow rate $q_J$ of the injector as a function of the percentage of flow removed in the first diffuser. It does not show the maximum expected.

## 5. Conclusion

The tests carried out on the $T'_2$ wind tunnel have shown that the injection system with vanes at the first elbow led to good performance of the system, that is to say, to a correct drive level for the principal flow ($Q_J$ / $Q_V$ ≈ 7.5). This result was arrived at through a variety of research bearing principally on the removal of the flow through the porous partition walls of the first diffuser situated through the flow region and the injector elbow.

Further progress is still possible, notably through the intake of a part of the injected flow at the level of the elbow so as to reduce the secondary effects. On the other hand, the attachment to to $T'_2$ of a transonic flow region with perforated or sintered partition walls will make it possible to determine the influence of the discharge flow in the plenum chamber and of the load losses of a mock-up unit on performance.

## REFERENCES


1. Carriere, P., Lecture series on "Large Transonic Wind Tunnels," Von Karman Institute, January 1973.

2. Schmitt, V., "Experimental Study of Internal Noise in Induction Wind Tunnels," Aerospace Research No. 1973-6 (Nov.-Dec.).

## Theory of Injectors

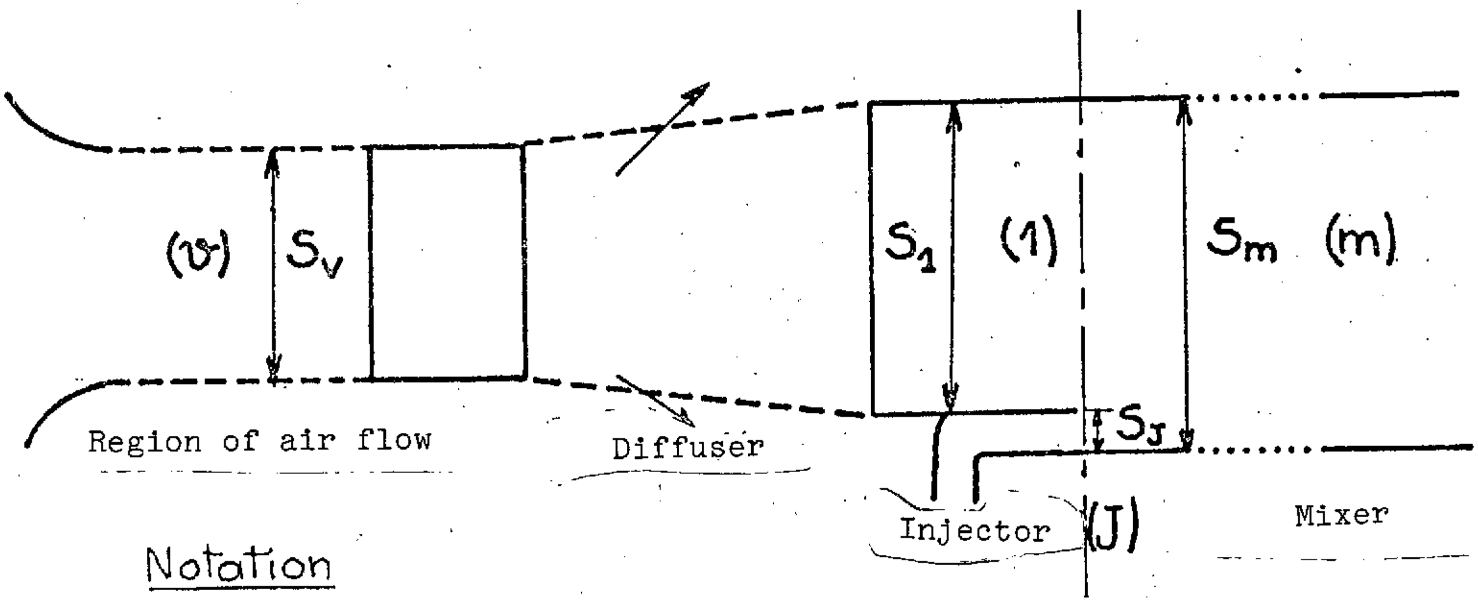


### Notation

$$\lambda = \frac{S_m}{S_J} \qquad \tau = \frac{1}{\lambda}$$

(v) $P_{iv}, P_v, M_v, \rho_v$
(1) $P_{i1}, P_1, M_1, \rho_1$
(J) $P_{iJ}, P_J, M_J, \rho_J$
(m) $P_{im}, P_m, M_m, \rho_m$

Uniform Flow

No losses at the partition walls

$h_{iJ} = h_{i1}$

### Conservation laws

Mass $\Longrightarrow (1-\tau)\rho_1 u_1 + \rho_J u_J \tau = \rho_m u_m$

Momentum $\Longrightarrow (1-\tau)(P+\rho u^2)_1 + \tau(P+\rho u^2)_J = (P+\rho u^2)_m$

Energy $\Longrightarrow h_{i1} = h_{iJ} = h_{im}$

Definition $\quad \mu^{-1} = \dfrac{\rho_J u_J \tau}{\rho_1 u_1 (1-\tau)} = \dfrac{q_{mJ}}{q_{m1}}$

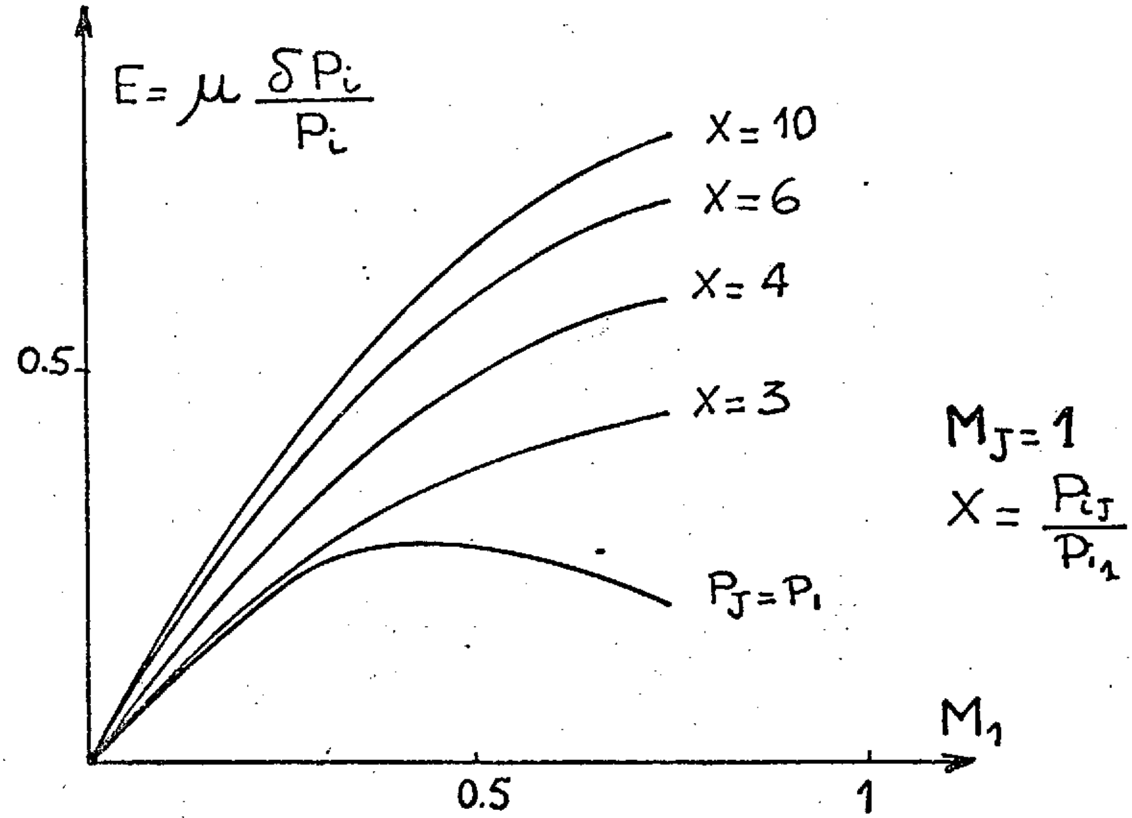


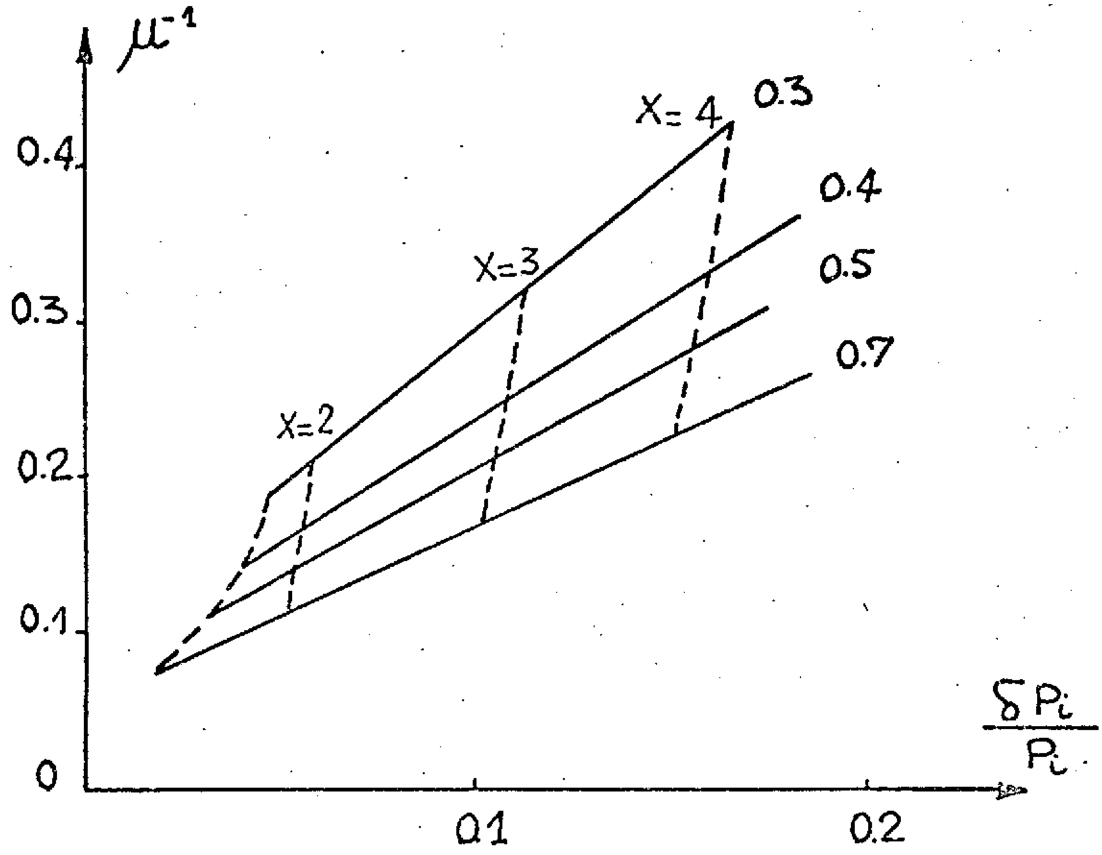


Performance of the Injectors



λ-20

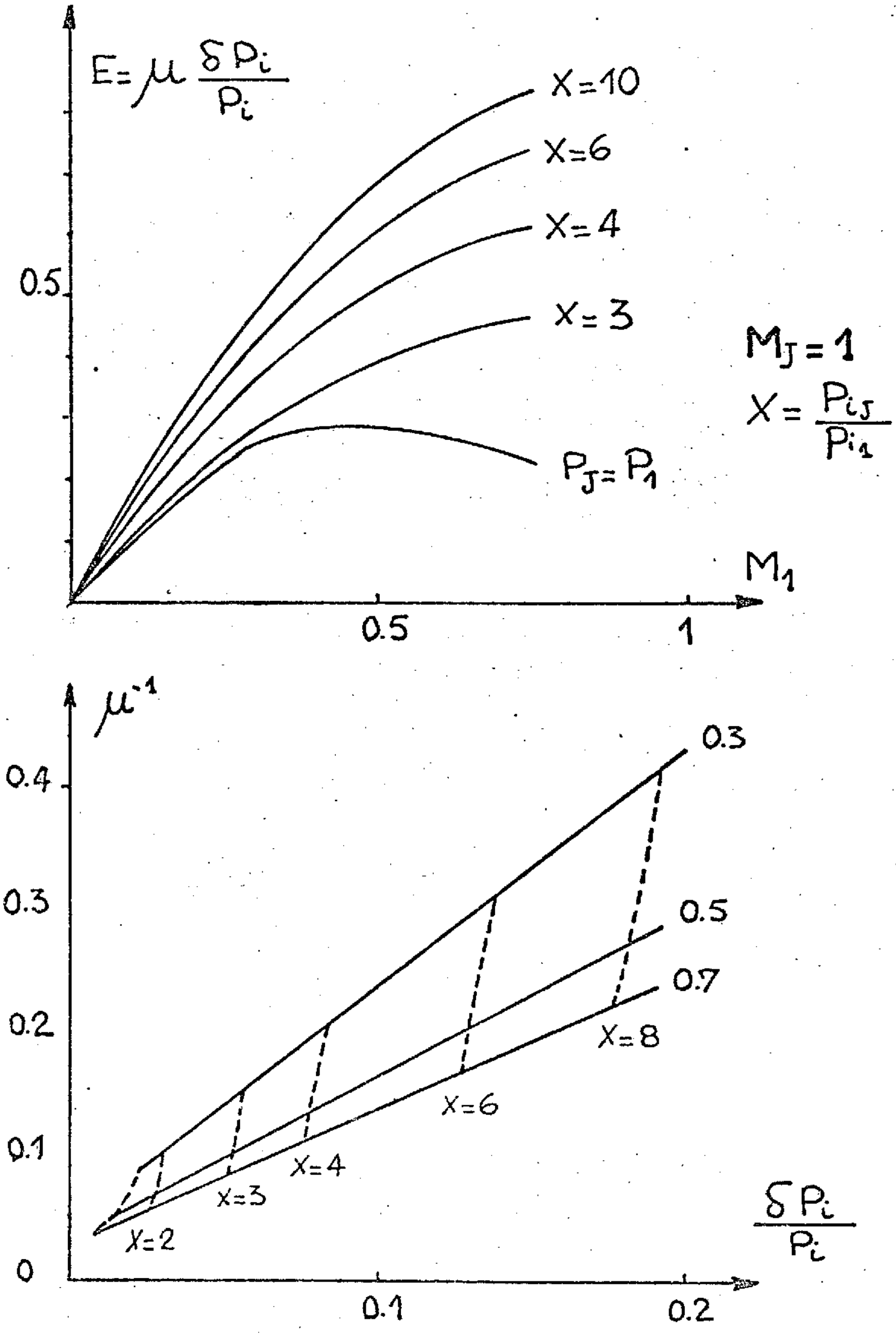


Performance of the Injectors

λ - 40

$\lambda = 20$

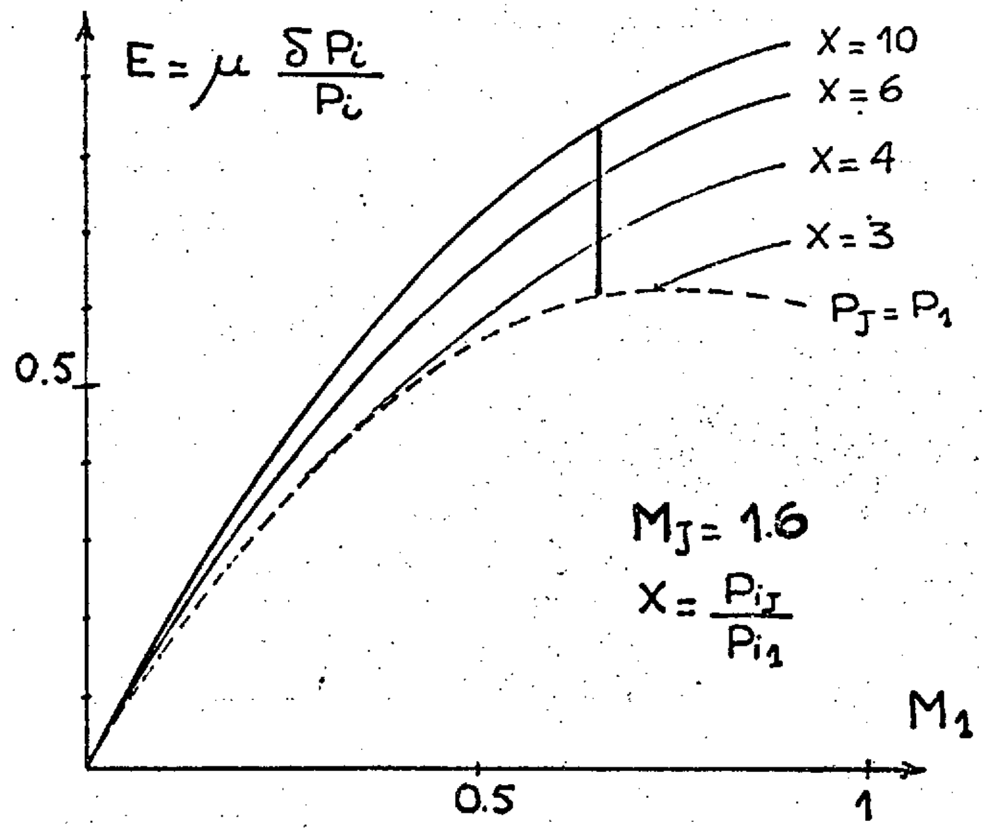
E = μ δPi/Pi
X = 10
X = 6
X = 4
X = 3
PJ = P1
0.5
MJ = 1.6
X = PiJ/Pi1
M1
0.5
1

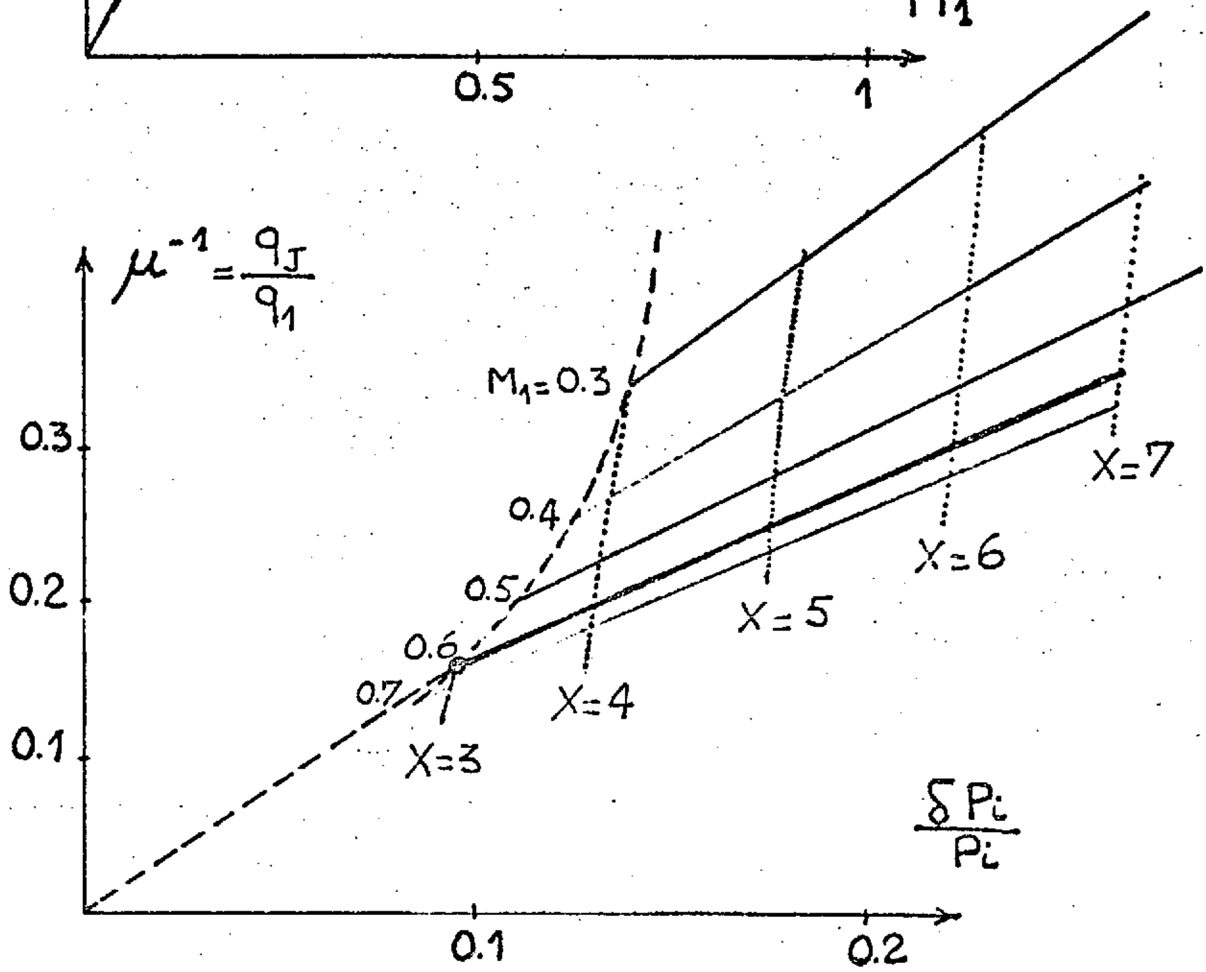
μ⁻¹ = qJ/q1
M1 = 0.3
0.4
0.5
0.6
0.7
0.3
0.2
0.1
X = 3
X = 4
X = 5
X = 6
X = 7
δPi/Pi
0.1
0.2

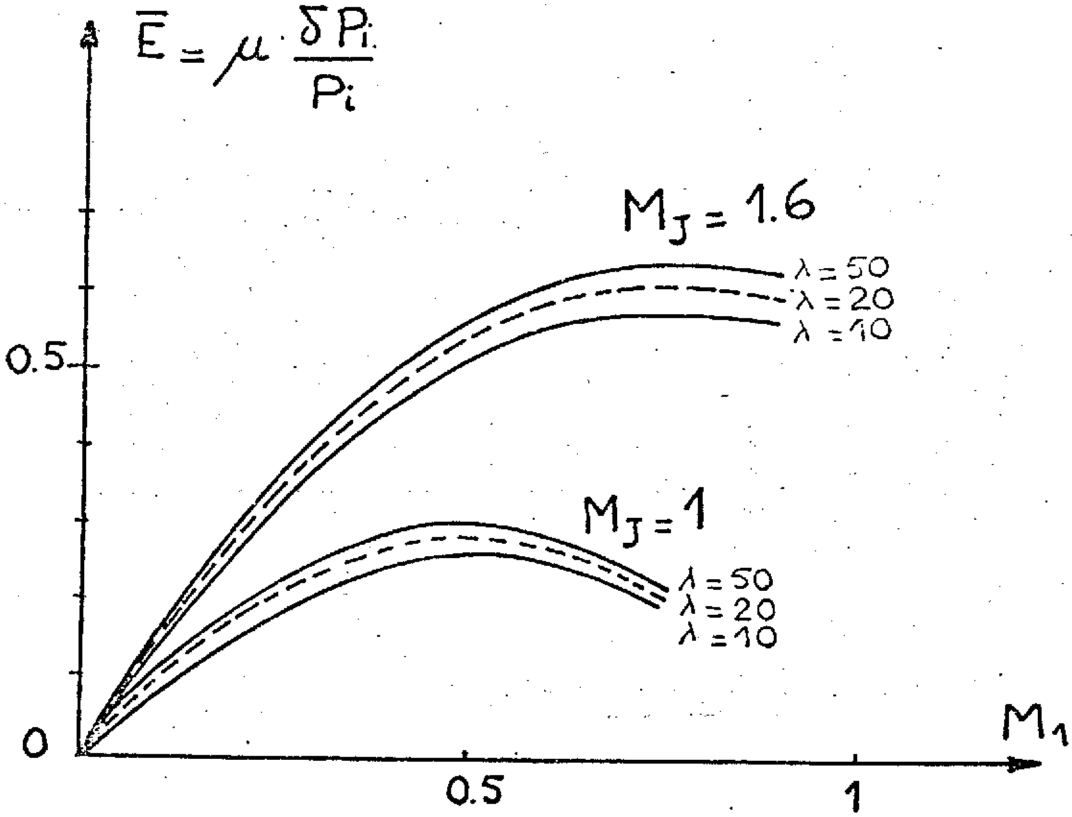


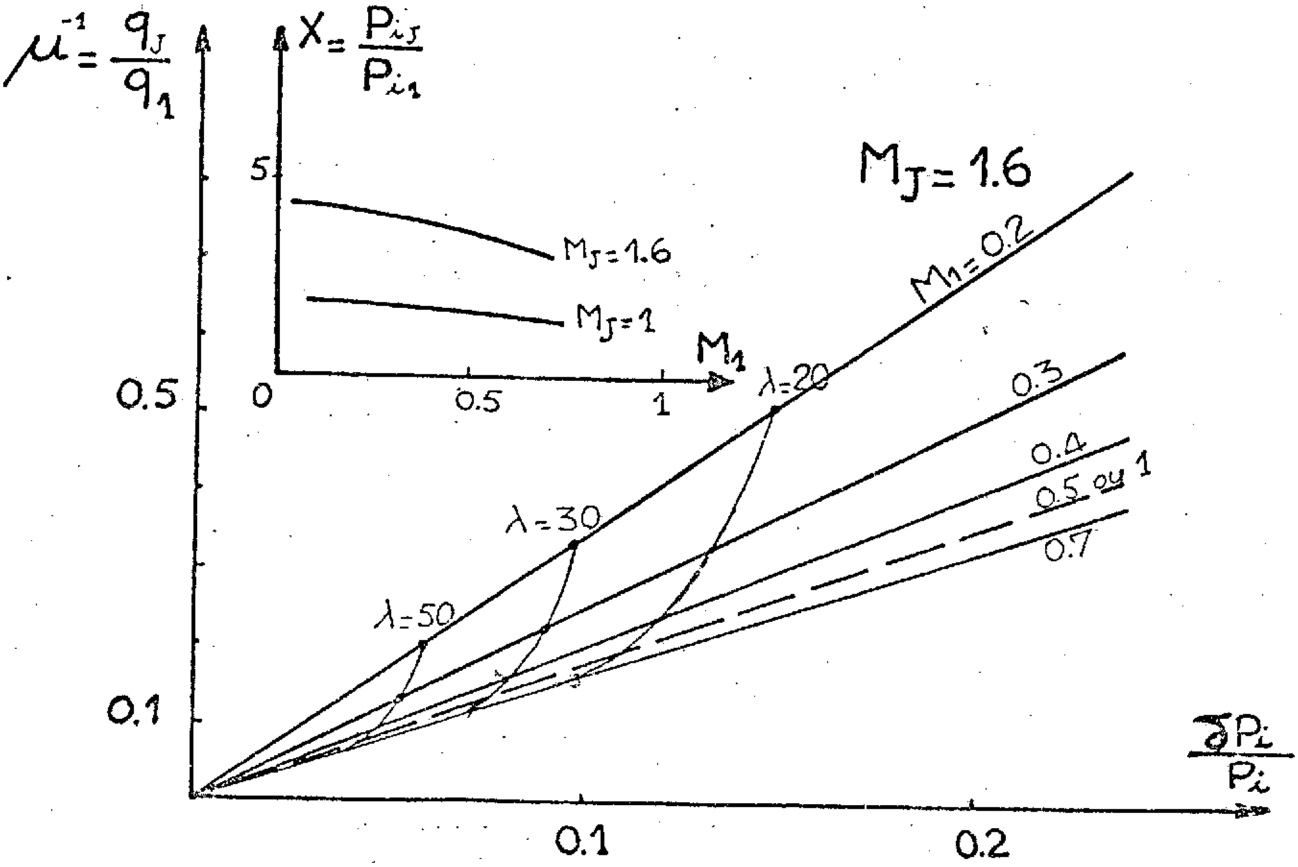


Performance of the Injectors

(Case of the Adjustment $P_J = P_1$)

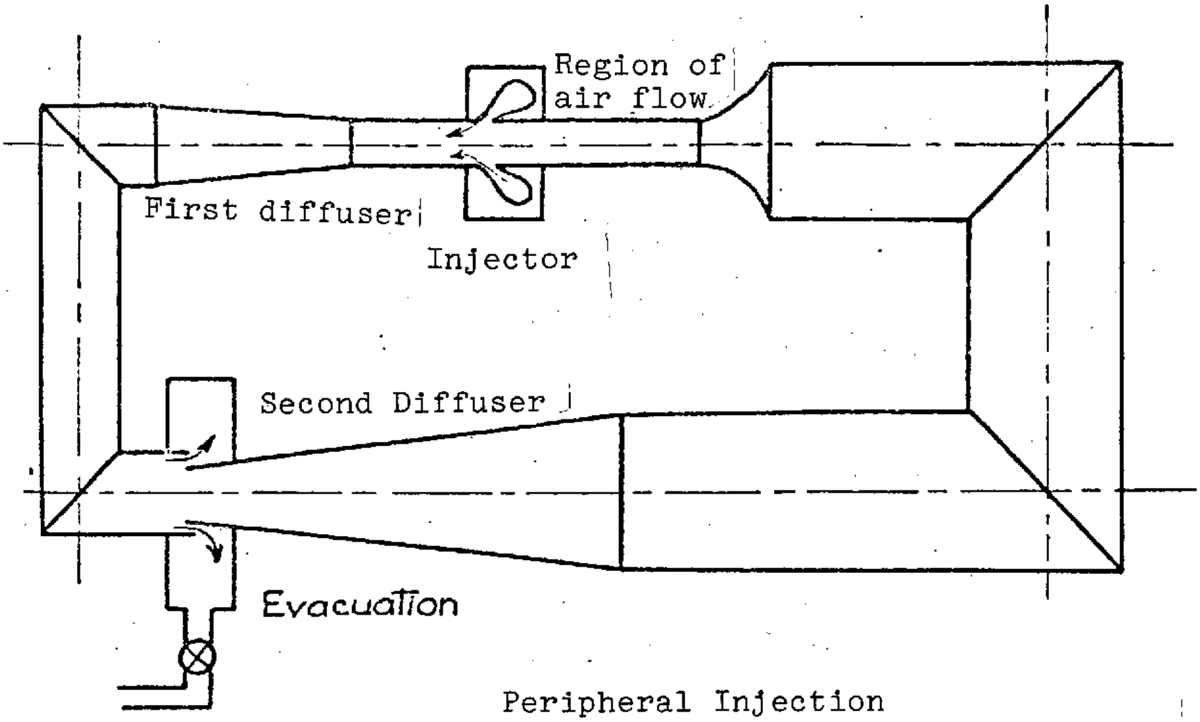


Peripheral Injection

Elbow Injection

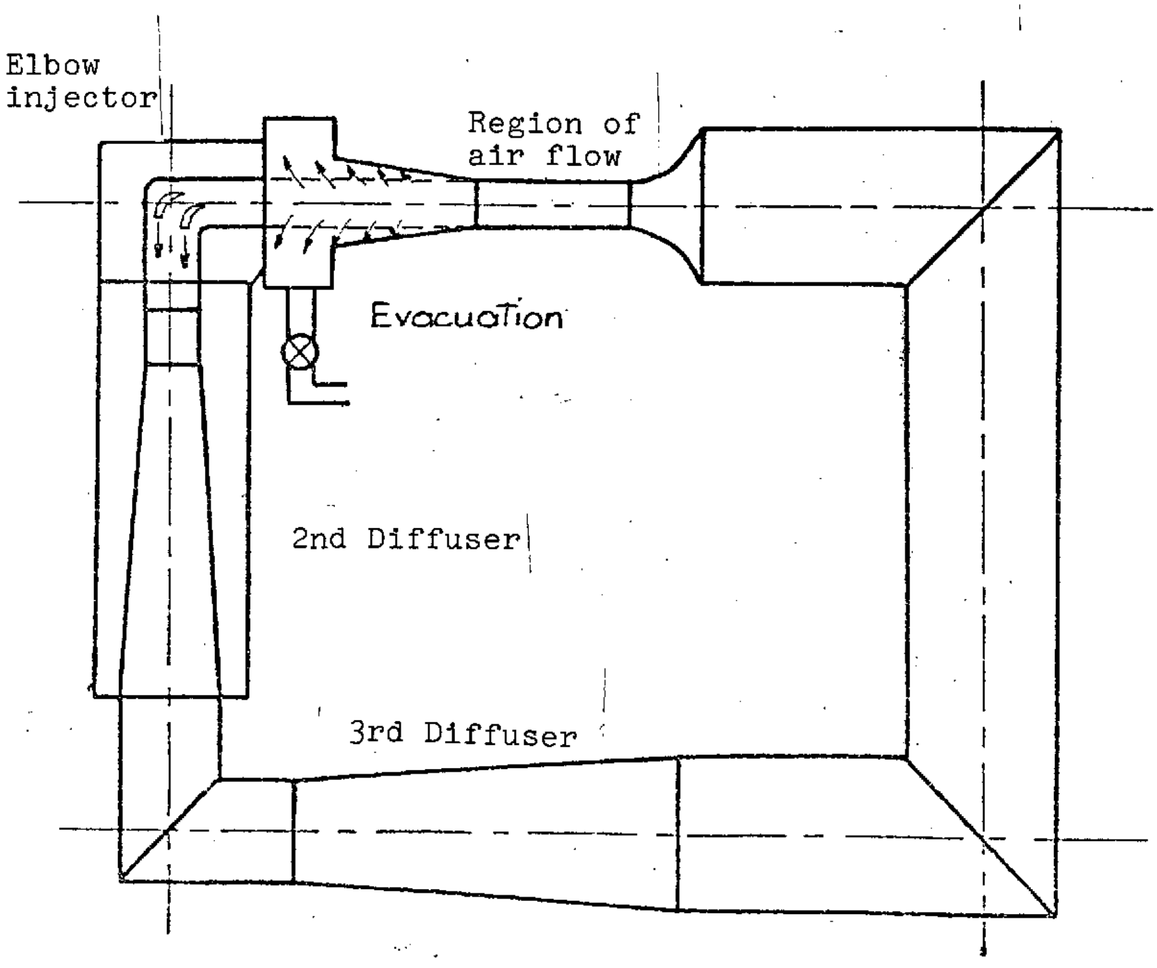

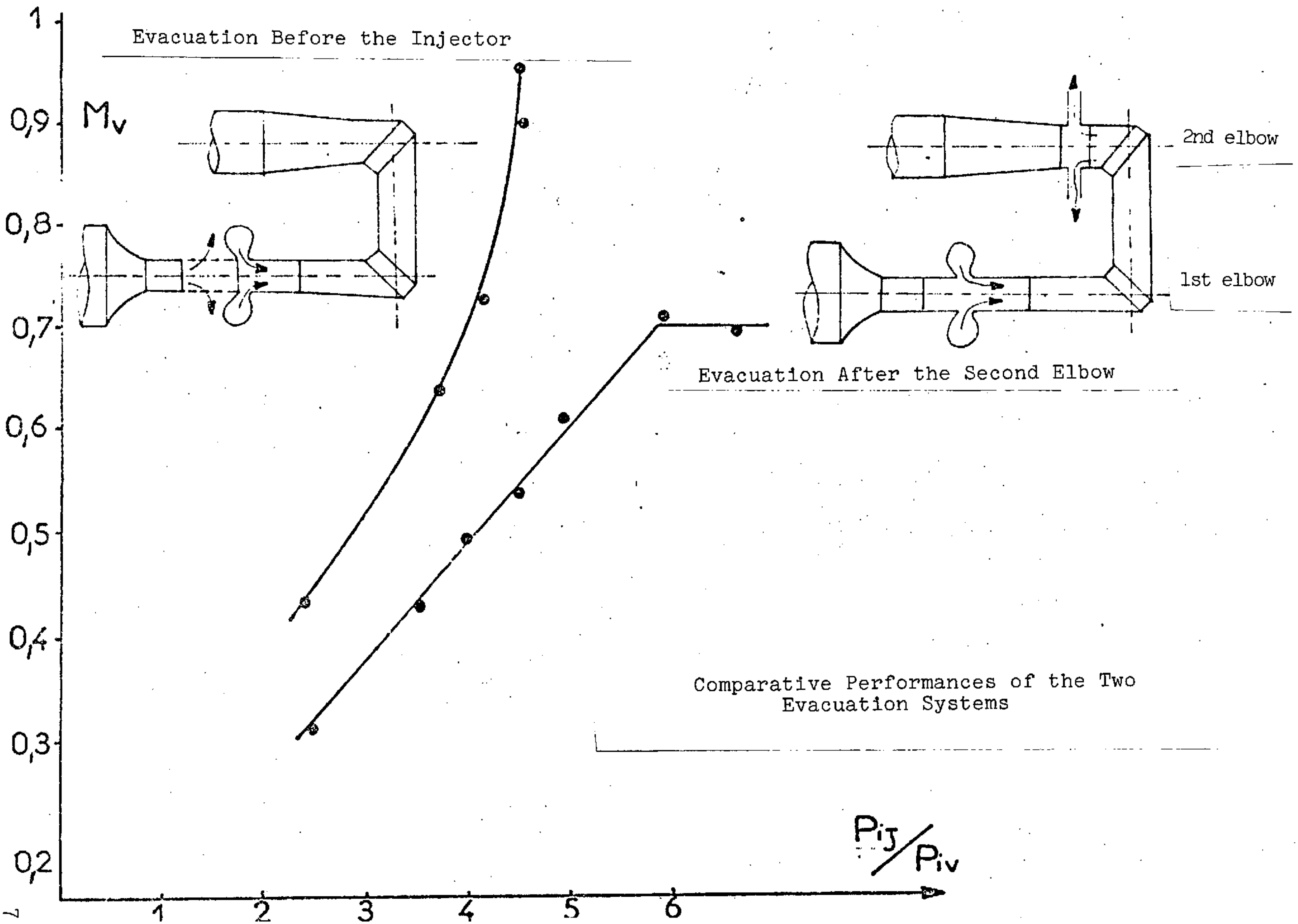
Evacuation Before the Injector
$M_v$
1
0,9
0,8
0,7
0,6
0,5
0,4
0,3
0,2
2nd elbow
1st elbow
Evacuation After the Second Elbow
Comparative Performances of the Two Evacuation Systems
$P_{iJ}/P_{iv}$
1
2
3
4
5
6

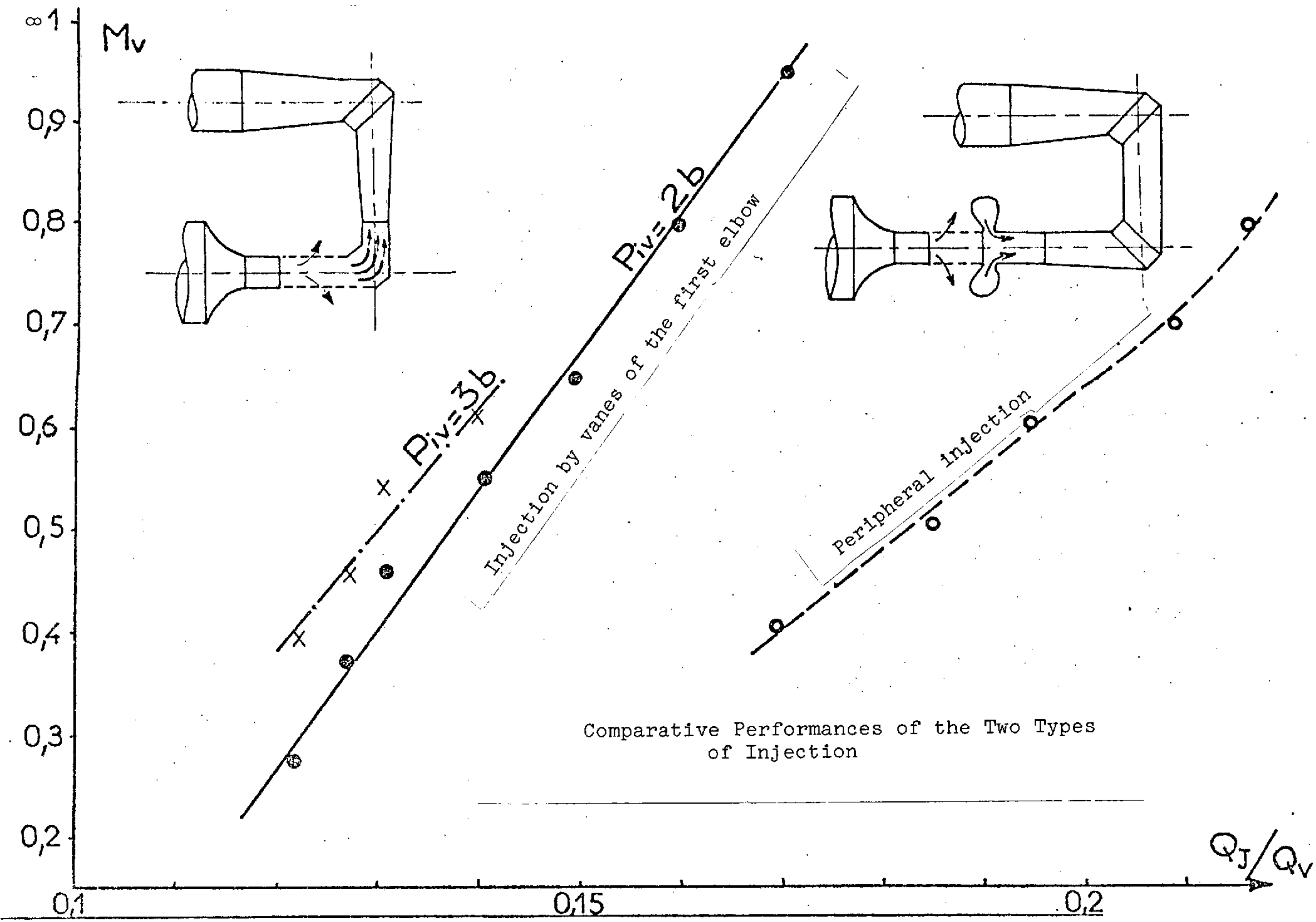


Comparative Performances of the Two Types of Injection

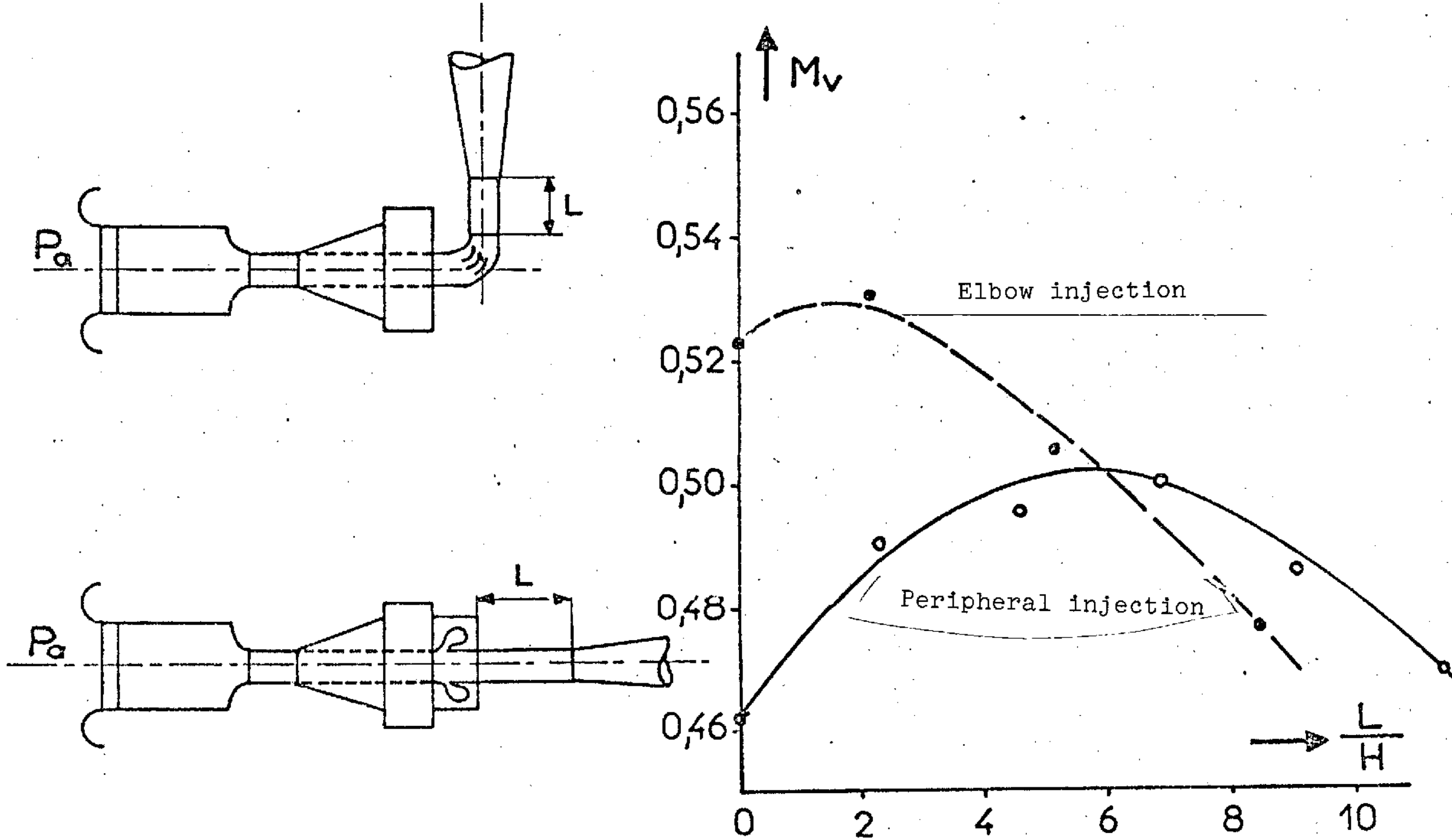


Influence of the Length of the Mixer

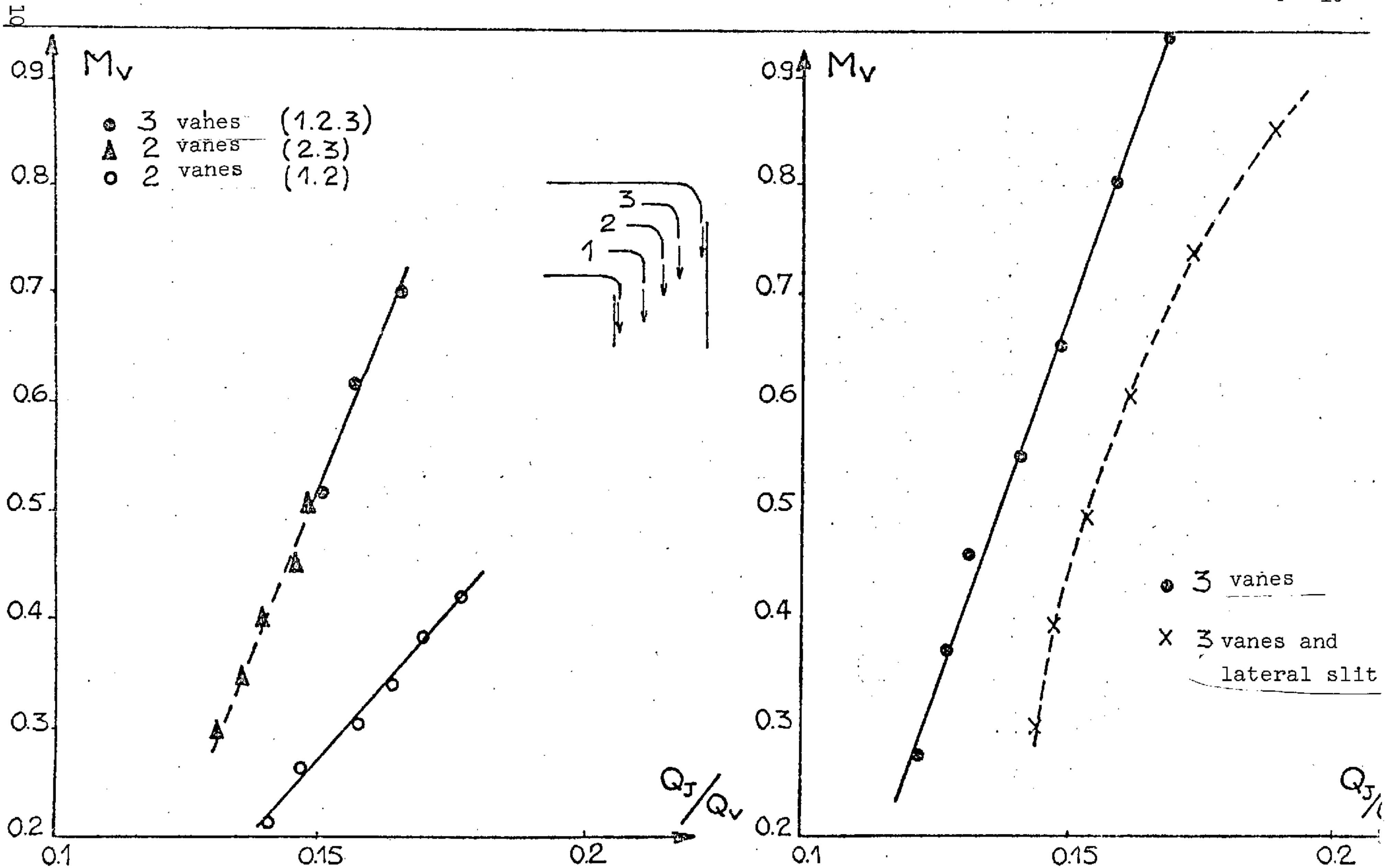


Efficiency of the Different Vanes and of the Lateral Slits

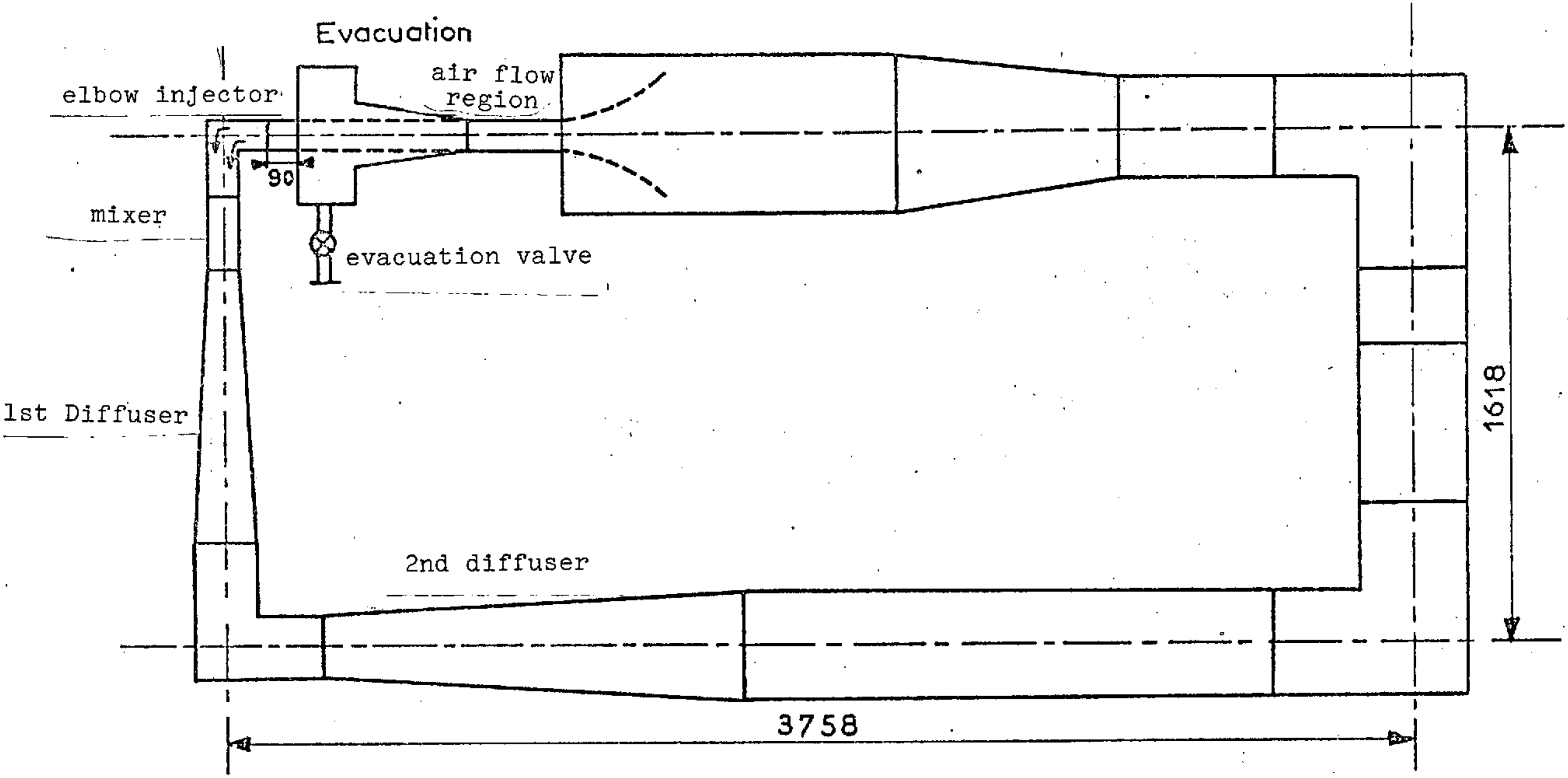


T'₂ Circuit Diagram
Elbow Injection

11

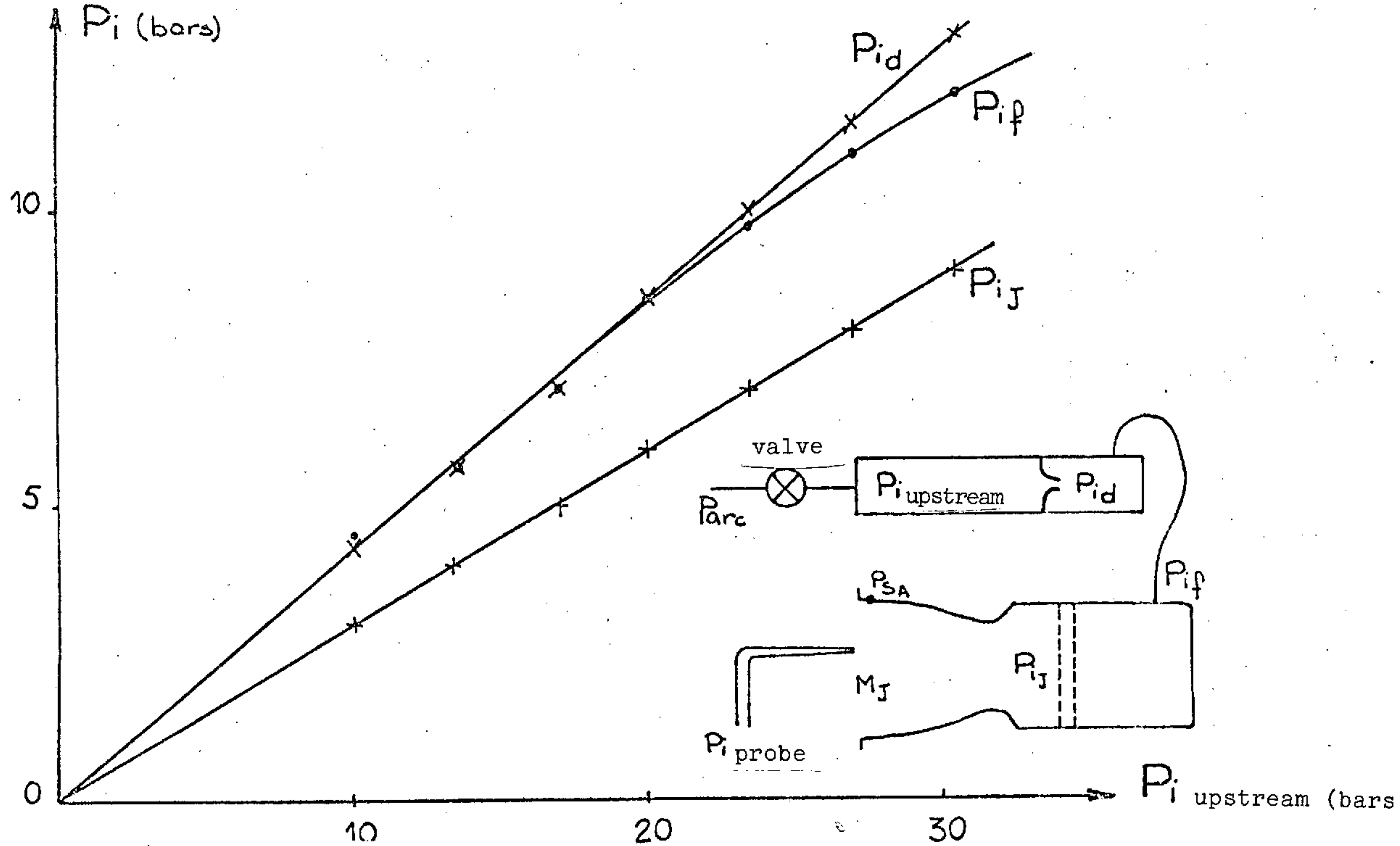


Impact Pressure Along the Feed Circuit

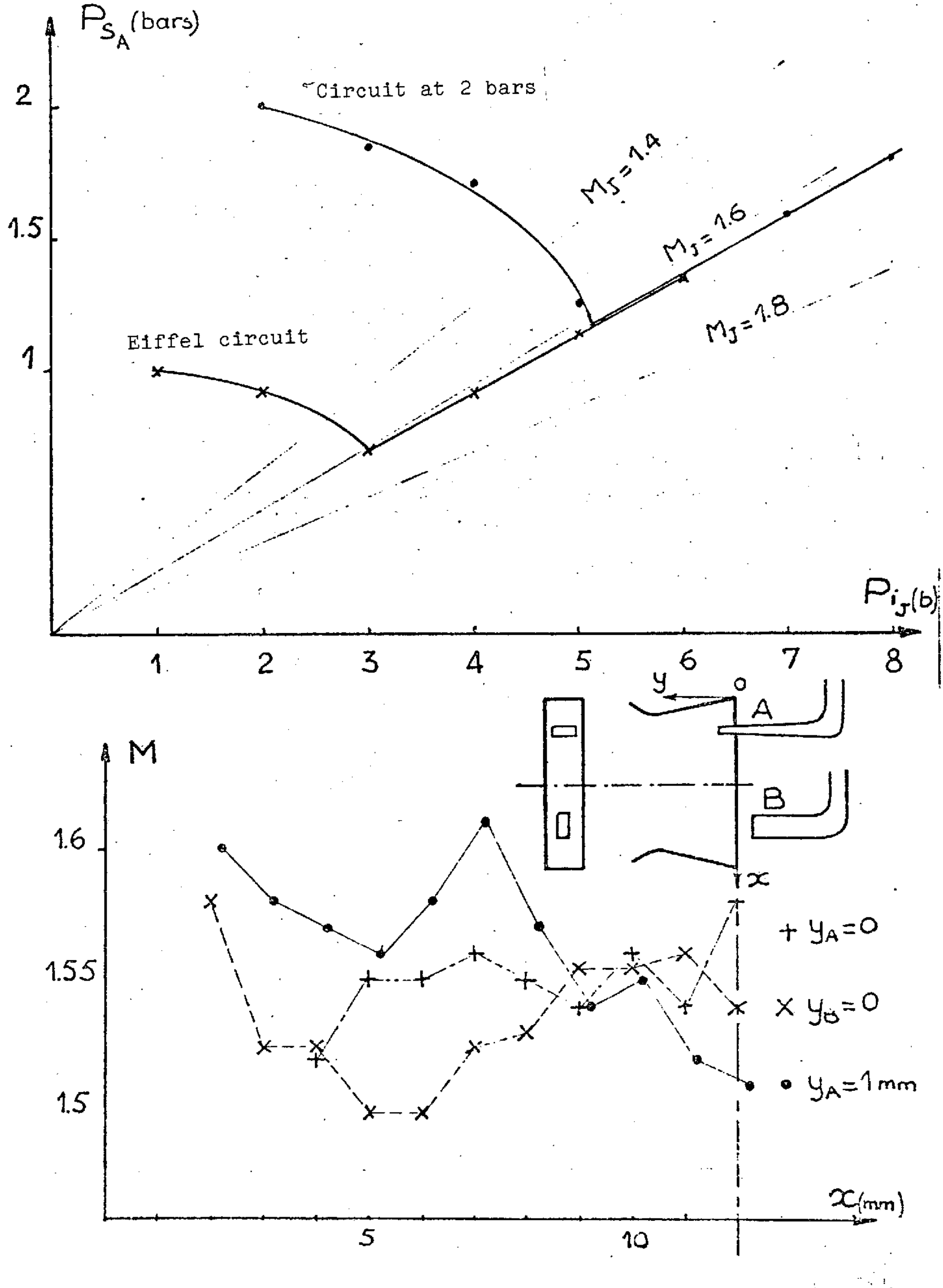


Measurement of the Injection Mach Number

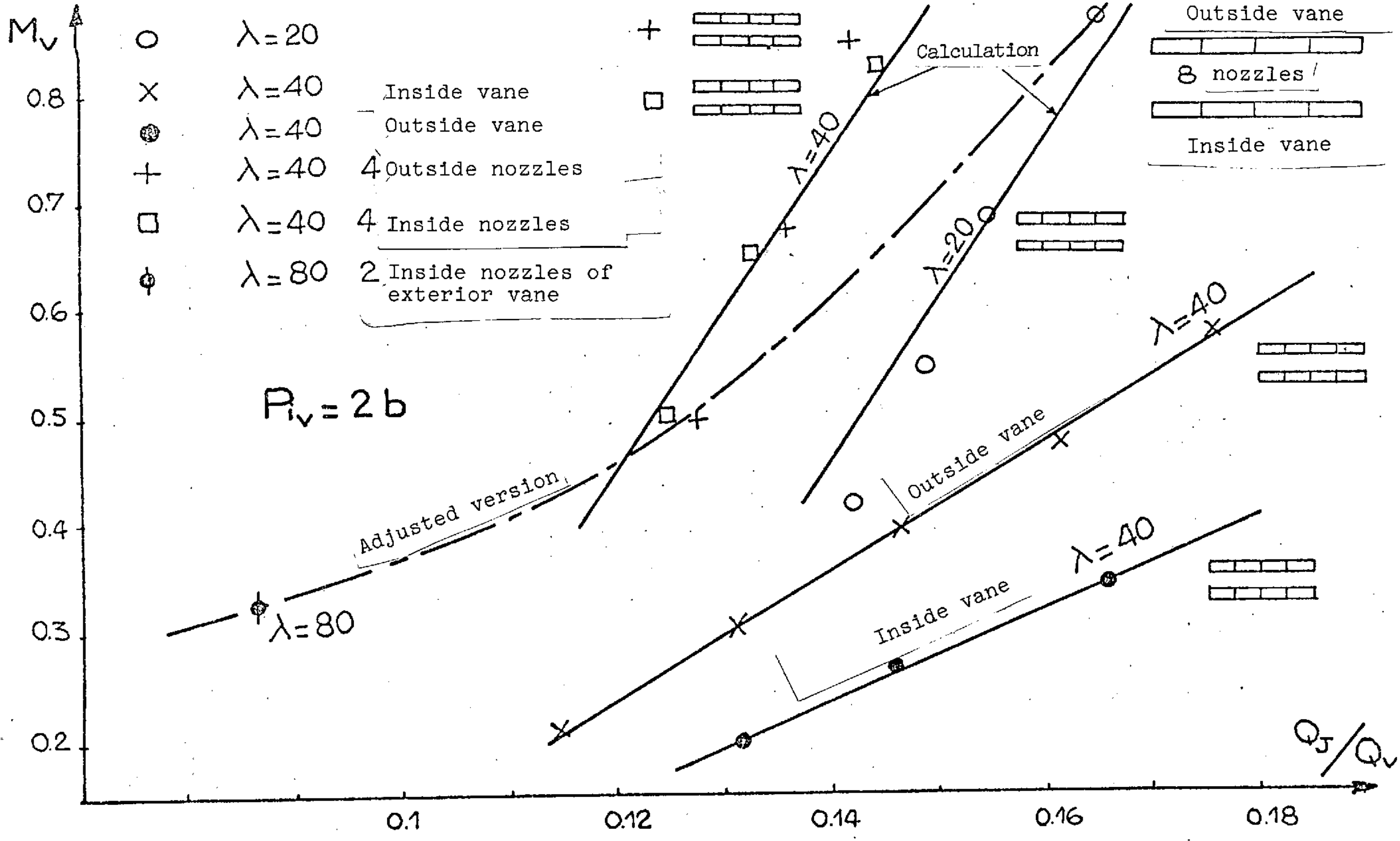


Performance of T'₂ with Variation of λ

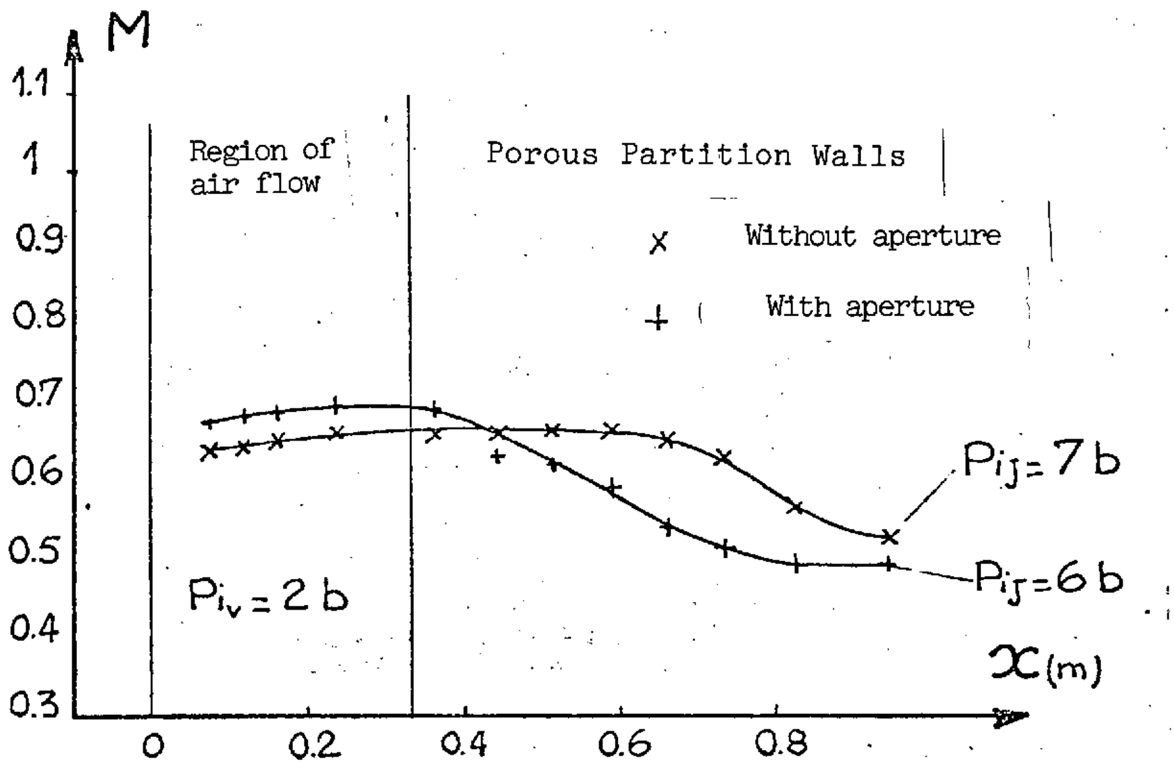


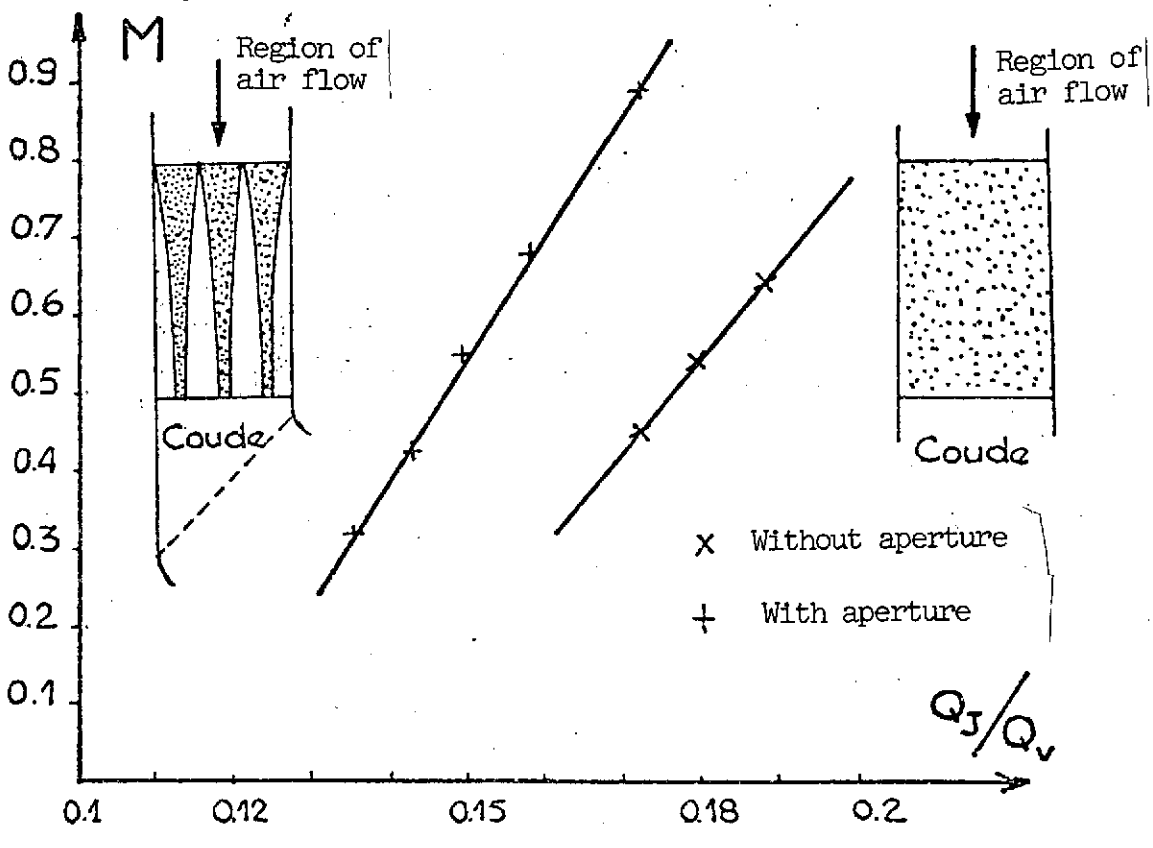


Effect of Apperture on Performance

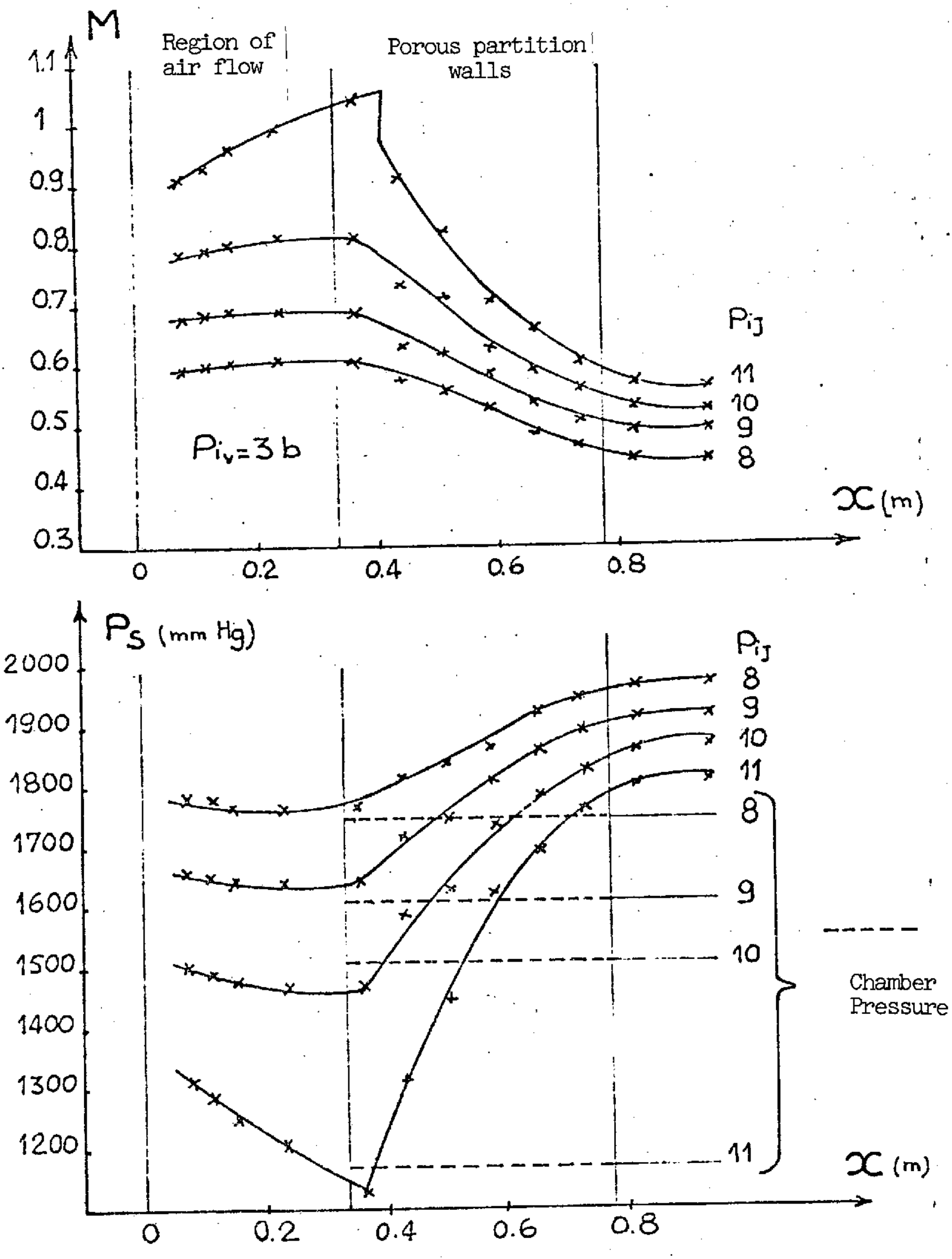


Operation of the Airflow – First Diffuser Elements

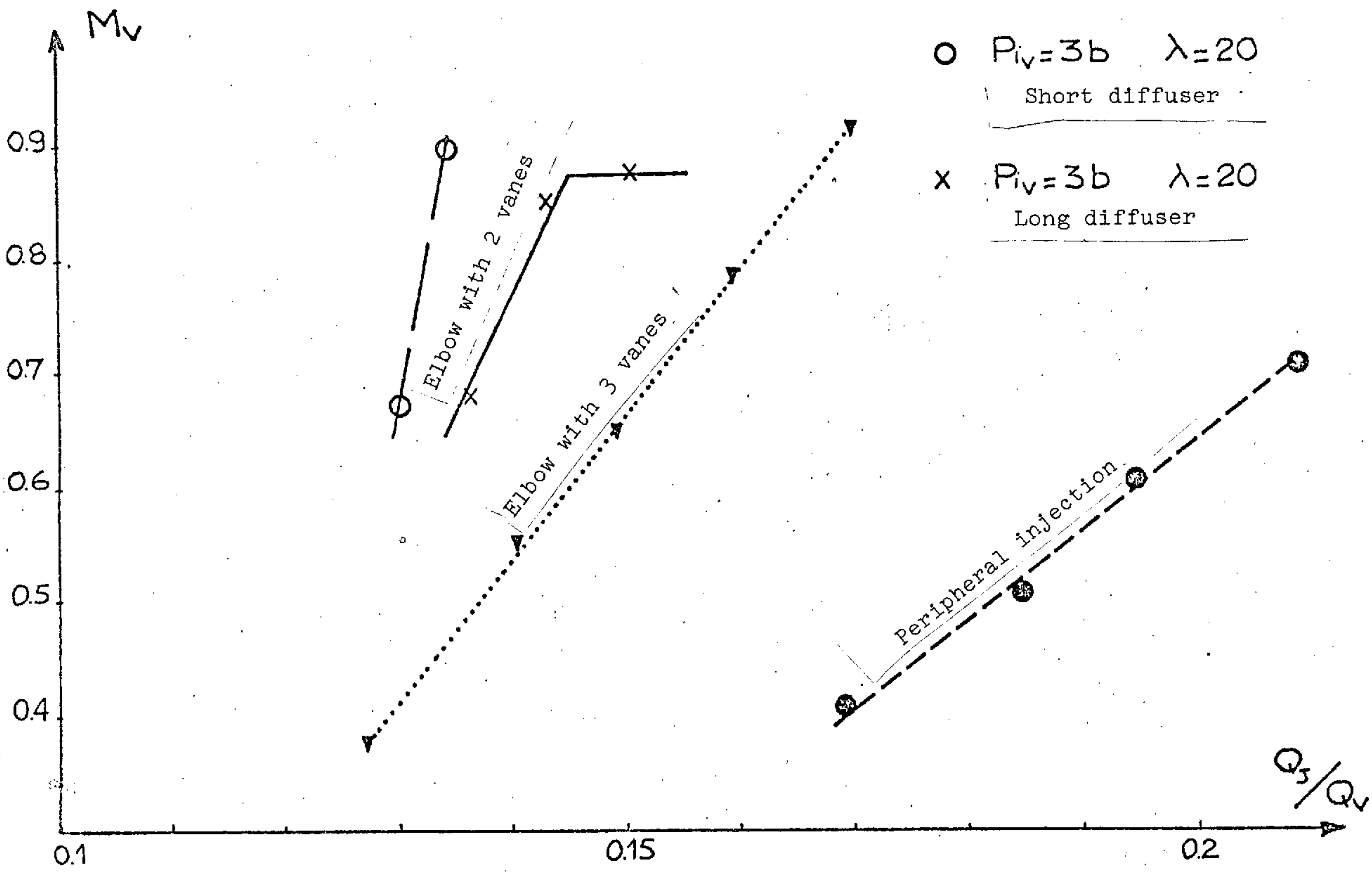




Improvement of Performance

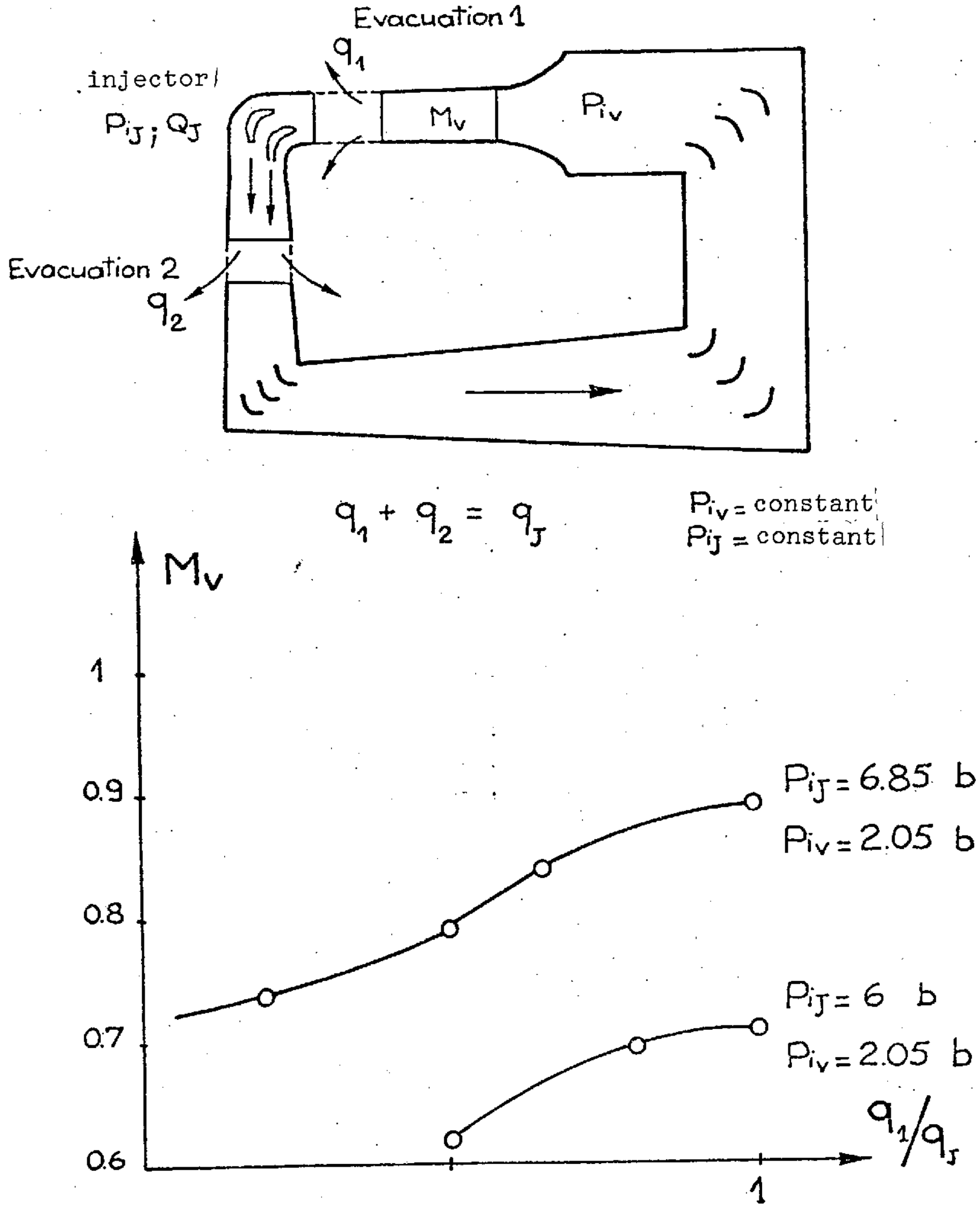


Influence of the Distribution of Evacuation Routes